Dehydration of the nanoporous coordination framework $Er^{III}[Co^{III}(CN)_6]\cdot 4(H_2O)$: single crystal to single crystal transformation and negative thermal expansion in $Er^{III}[Co^{III}(CN)_6]$†

Thorsten Pretsch, Karena W. Chapman, Gregory J. Halder and Cameron J. Kepert*

Received (in Cambridge, UK) 27th January 2006, Accepted 6th March 2006
First published as an Advance Article on the web 20th March 2006
DOI: 10.1039/b601344a

Desorption of bound and unbound water molecules from the nanoporous coordination framework $Er^{III}[Co^{III}(CN)_6]\cdot 4H_2O$ to form the apohost, $Er^{III}[Co^{III}(CN)_6]$, proceeds *via* a single crystal to single crystal transformation in which the Er(III) cations change from 8- to 6-coordinate; dehydration results in a striking change in the thermal expansion properties.

Materials exhibiting negative thermal expansion (NTE) have received considerable recent attention due both to their fundamental and commercial interest.[1] Among flexible NTE systems such as oxide-bridged (M–O–M′)[2,3] and cyanide-bridged (M–CN–M′)[4–6] frameworks, NTE behaviour has been attributed to the existence of low-energy transverse vibrational modes of the bridging species. These vibrations typically have an effect over wide temperature ranges and in certain cases have been shown to be coupled throughout the lattice as rigid unit modes (RUMs)[7] involving the cooperative dynamic rotation of metal centres. In the oxide-bridged phase ZrW_2O_8, for example, there is an increasing concerted rotation of the rigid ZrO_6 octahedra and WO_4 tetrahedra with increasing temperature.[3] In the considerably more flexible cyanide-based phases such as $Zn_xCd_{1-x}(CN)_2$ ($0 \leqslant x \leqslant 1$), the neighbouring metal centres are effectively decoupled in their relative rotation and translation due to the greater flexibility of the double-atom cyanide bridge.[4]

Among cyanide-bridged NTE systems, the nanoporous Prussian Blue analogues $MPt(CN)_6\cdot x(H_2O)$ (M = Zn, Cd; x = 0, 2) have recently been shown to display guest-dependent NTE; removal of unbound water from each of the hydrated Zn and Cd analogues causes subtle changes to the thermal expansion properties.[5] Here we extend our interest in such behaviour to a member of the lanthanoid(III) hexacyanometallate(III) hydrate family, $Er^{III}[Co^{III}(CN)_6]\cdot 4H_2O$, which contains both bound and unbound water. The results of variable temperature single crystal X-ray diffraction experiments on both the hydrated and dehydrated phases are presented.

The structures of the lanthanoid(III) hexacyanometallate(III) hydrates, $Ln^{III}[M^{III}(CN)_6]\cdot xH_2O$ (Ln = lanthanoid; M = transition metal; x = 4, 5), consist of alternating, cyanide-bridged MC_6 and LnN_6O_y (y = 2, 3) polyhedra and are either orthorhombic or hexagonal in symmetry depending on the degree of hydration at the lanthanoid centre.[8] In the orthorhombic phase $Er[Co(CN)_6]\cdot 4H_2O$ (**A·4H$_2$O**), two water molecules are bound to each Er atom and two further uncoordinated water molecules occupy 3D channels within the lattice.

Following the collection of variable temperature unit cell and full-sphere crystallographic data on a fresh crystal of **A·4H$_2$O**,‡§ the same crystal was heated *in-situ* during X-ray diffraction data collection to 450 K under dry dinitrogen to convert it to the dehydrated material, **A**.[9] Analysis of the resulting data indicated a retention of monocrystallinity with no observable increase in crystal mosaicity. The transformation results in a dramatic change to the framework structure and a conversion from orthorhombic *Cmcm* (**A·4H$_2$O**) to hexagonal $P6_3/mmc$ (**A**) symmetry (Fig. 1(a),(b)); this corresponds to an effective tripling of the crystallographic symmetry.§ Notably, the removal of the two bound water molecules from the Er centre is accompanied by a transformation of the Er coordination geometry from bicapped trigonal prismatic (C_{2v} symmetry) to trigonal prismatic (D_{3h}) (Fig. 1(c),(d)). Comparison of structural data of **A·4H$_2$O** and **A** at 100, 150, 225, 300 and 375 K indicates that the Er coordination sphere contracts considerably following dehydration; at 100 K, the average Er–N bond distance decreases from 2.432 to 2.332 Å. There are no significant accompanying changes to the C–N and Co–C distances. We note that trigonal prismatic coordination is

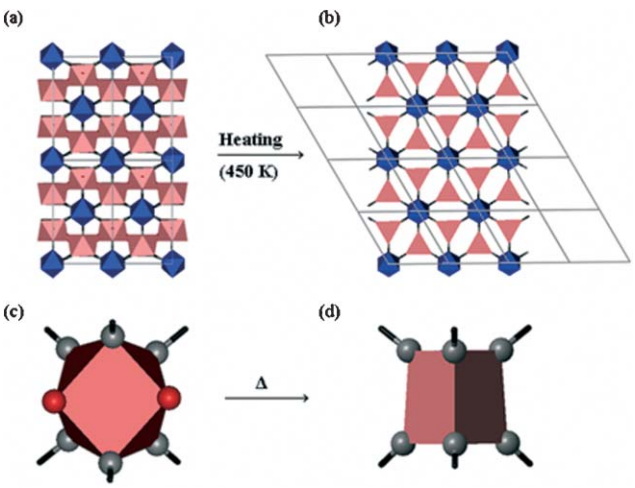

Fig. 1 Polyhedral representation of the single crystal to single crystal transformation from **A·4H$_2$O** (a; unbound water removed for clarity) to **A** (b) (Er polyhedra red; Co octahedra blue, C black, O red and N grey). Dehydration results in a change in the Er coordination geometry from 8-coordinate bicapped trigonal prismatic (ErN_6O_2) (c) to 6-coordinate trigonal prismatic (ErN_6) (d).

School of Chemistry, University of Sydney, Australia.
E-mail: c.kepert@chem.usyd.edu.au; Fax: +61 2 9351 3329;
Tel: +61 2 9351 5741

† Electronic supplementary information (ESI) available: Experimental details and crystallographic data. See DOI: 10.1039/b601344a

highly unusual for 6-coordinate trivalent lanthanoids, for which octahedral coordination is generally preferred (as seen, for example, in the anhydrous lanthanoid halides).[10] This unusual arrangement may be forced by the geometric constraint of the framework; such a constraint arises with the network connectivity being retained following the topotactic transformation, rather than converting to other, potentially more stable topologies such as the Prussian Blue lattice type.

Comparison of the variable temperature unit cell data reveals that **A** displays near-isotropic NTE from 100 to 375 K, with $\alpha_a = \mathrm{d}a/a\mathrm{d}T = -8 \times 10^{-6}\ \mathrm{K}^{-1}$, $\alpha_c = -9 \times 10^{-6}\ \mathrm{K}^{-1}$ and $\alpha_l = 1/3\ \mathrm{d}V/V\mathrm{d}t = -9 \times 10^{-6}\ \mathrm{K}^{-1}$ (Fig. 2). The intermediate magnitude of the thermal expansion coefficients relative to those of the $M(CN)_2$[4] and $M^{II}Pt^{IV}(CN)_6$[5,11] phases is consistent with the intermediate average metal–cyanide bond energies of this material, supporting the view that thermal population of low energy transverse vibrations of the cyanide bridges is principally responsible for the NTE behaviour. Calculations within PLATON[12] reveal that 31.7% of the unit cell is void and thus free space for such vibrations.

Examination of the anisotropic thermal displacement parameters reveals a progressive elongation of the thermal ellipsoids of the cyanide atoms perpendicular to the Co···Er axis with increasing temperature (Fig. 3). In considering the influence of the low energy transverse vibrations of the cyanide bridge, it is pertinent to note that this phase is unique among known cyanide-based NTE systems in having non-linear M–CN–M′ linkages. As such, both the vibrational amplitude and any net translation and rotation of the cyanide unit towards or away from the M···M′ axis will influence the M···M′ separation. Comparison of the Co···Er distances shows that this phase behaves like the linear M–CN–M′ systems in that the metal centres are drawn progressively closer together with increasing temperature: the crystallographic Co···Er distance decreases from 5.3695(2) Å at 100 K to 5.3568(2) Å at 375 K.

As with the $M(CN)_2$ and Prussian Blue families,[4] the transverse cyanide vibrations can be coupled to form volume-reducing

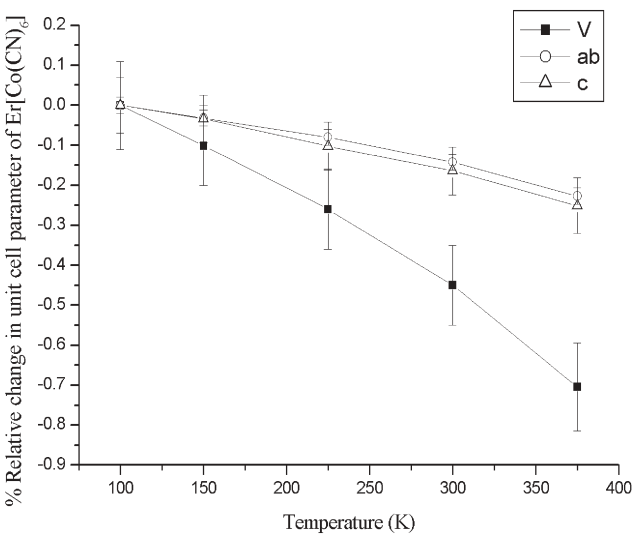

Fig. 2 Temperature-dependent unit cell parameters of **A**, as determined by single crystal X-ray diffraction. Values are given relative to those at 100 K. Error bars are ±1 e.s.d.

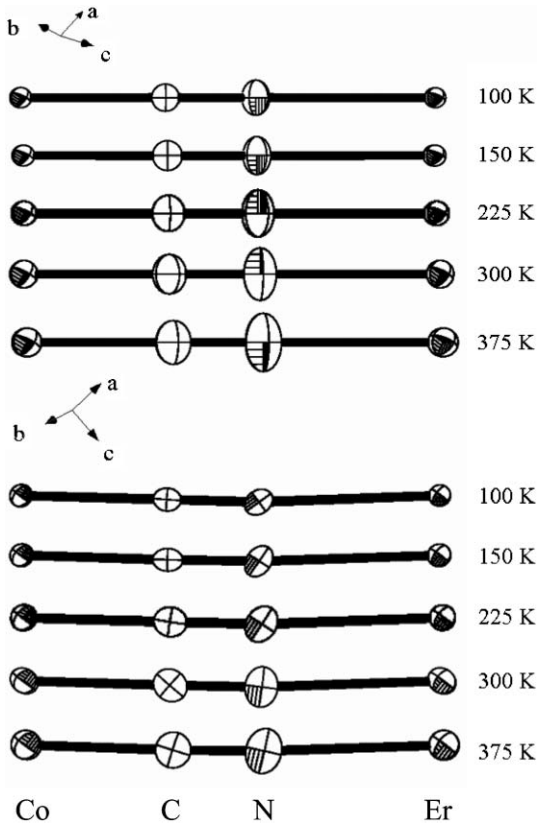

Fig. 3 Orthogonal perspectives of the temperature-dependent thermal ellipsoids of the asymmetric unit of **A**, drawn with 50% probability level.

RUMs of CoC_6 and ErN_6 polyhedra (see Fig. 4 for a representation of two simple RUMs for this structure). An intriguing feature that distinguishes this framework from other oxide- and cyanide-bridged NTE materials, however, is the presumed relative instability of the trigonal prismatic coordination geometry about the Er centre. It seems likely that dynamic deviations from this geometry towards the trigonal antiprismatic arrangement (akin to eclipsed towards staggered) may occur at relatively low energy, raising the possibility that 'non-rigid unit' motion about this centre may contribute significantly to the observed NTE.

In contrast to **A**, the hydrated material **A·4H$_2$O** displays positive thermal expansion (PTE) with $\alpha_V = +11 \times 10^{-6}\ \mathrm{K}^{-1}$ (Fig. S1). We attribute this property principally to an increase in kinetic volume of the bound and unbound water molecules with increasing temperature; a similar steric effect involving unbound

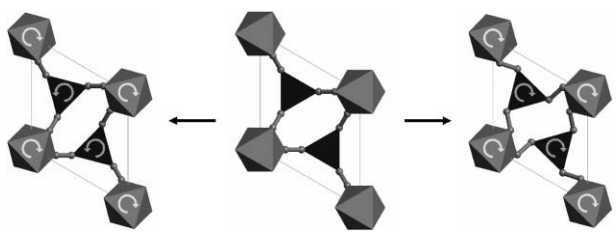

Fig. 4 Schematic representation of two possible low energy rigid unit modes involving rotation of CoC_6 and ErN_6 coordination polyhedra in **A**; each mode leads to a reduction in crystal volume.

This journal is © The Royal Society of Chemistry 2006

water only has recently been seen in $ZnPt(CN)_6 \cdot x(H_2O)$ ($x = 0, 2$).[5] The presence of distinctly non-linear M–CN–M′ linkages may also favour PTE in this phase. The average crystallographic Co···Er distance increases from 5.296 Å at 100 K to 5.322 Å at 375 K, with an accompanying straightening of the average Er–N–C and Co–C–N angles from 157.9° to 159.8° and 178.8° to 179.0°, respectively.

In summary, we demonstrate that dehydration of $Er[Co(CN)_6] \cdot 4(H_2O)$ occurs *via* a remarkable single crystal to single crystal transformation. The dehydrated phase, $Er[Co(CN)_6]$, exhibits pronounced NTE and is notable both in having an unusual lanthanoid coordination geometry and a non-linear cyanide linkage between the metal centres.

This work was supported by the Australian Research Council. TP thanks the Deutsche Akademie der Naturforscher Leopoldina funded by the Bundesministerium für Bildung und Forschung (BMBF-LPD 9901/8-125) for a fellowship. We thank Dr P. Turner for assistance with the single crystal X-ray diffraction measurements.

Notes and references

‡ *Synthesis of* **A·4H$_2$O**: Crystals were grown by slow diffusion in aqueous solution. Three solutions were layered in a single 10 ml screw cap vial: 110.9 mg (0.25 mmol) $Er(NO_3)_3 \cdot 5H_2O$ in 0.5 ml H_2O; 300 mg (2.97 mmol) KNO_3 in 1 ml H_2O; and 83.1 mg (0.25 mmol) $K_3[Co(CN)_6]$ in 2 ml dist. H_2O. Pink crystals (76.7 mg) were filtered off after one week.

§ *Crystal data* of **A·4H$_2$O** at 100 K: $C_6H_8N_6ErCoO_4$, M = 454.37, orthorhombic, space group *Cmcm*, a = 7.2835(15), b = 12.584(3), c = 13.462(3) Å, V = 1233.8(4) Å^3, Z = 4, D_c = 2.446 g cm^{-3}, μ = 8.115 mm^{-1}, F(000) = 820, 4247 reflections measured, 835 unique (R_{int} = 0.0368). Final residuals (for 58 parameters) were $R1$ = 0.0297, $wR2$ = 0.0701. *Crystal data* of **A** at 100 K: C_6N_6ErCo, M = 382.31, hexagonal, space group $P6_3/mmc$, a = 7.3887(10), c = 13.044(3) Å, V = 616.69(17) Å^3, Z = 2, D_c = 2.059 g cm^{-3}, μ = 8.074 mm^{-1}, F(000) = 346, 8106 reflections measured, 415 unique (R_{int} = 0.0173). Final residuals (for 17 parameters) were $R1$ = 0.0117, $wR2$ = 0.0256. *Crystal data* of **A** at 375 K: C_6N_6ErCo, M = 382.31, hexagonal, space group $P6_3/mmc$, a = 7.3719(10), c = 13.011(3) Å, V = 612.35(17) Å^3, Z = 2, D_c = 2.073 g cm^{-3}, μ = 8.132 mm^{-1}, F(000) = 346, 7336 reflections measured, 412 unique (R_{int} = 0.0185). Final residuals (for 17 parameters) were $R1$ = 0.0124, $wR2$ = 0.0236. For crystallographic data of **A·4H$_2$O** (CCDC 296841–296845) and **A** (CCDC 296836–296840) at 100, 150, 225, 300 and 375 K in CIF or other electronic format see DOI: 10.1039/b601344a

1 J. S. O. Evans, *J. Chem. Soc., Dalton Trans.*, 1999, 3317–3326; A. W. Sleight, *Annu. Rev. Mater. Sci.*, 1998, **28**, 29–43; R. Roy, D. K. Agrawal and H. A. McKinstry, *Annu. Rev. Mater. Sci.*, 1989, **19**, 59–81; G. D. Barrera, J. A. O. Bruno, T. H. K. Barron and N. L. Allan, *J. Phys.: Condens. Matter*, 2005, **17**, 217–252; J. R. Salvador, F. Gu, T. Hogan and M. G. Kanatzidis, *Nature*, 2003, **425**, 702–705; J. Arvanitidis, K. Papagelis, S. Margadonna, K. Prassides and A. N. Fitch, *Nature*, 2003, **425**, 599–602; K. Takenaka and H. Takagi, *Appl. Phys. Lett.*, 2005, **87**, 261902.

2 V. Korthuis, N. Khosrovani, A. W. Sleight, N. Roberts, R. Dupree and W. W. Warren, *Chem. Mater.*, 1995, **7**, 412–417; T. A. Mary, J. S. O. Evans, T. Vogt and A. W. Sleight, *Science*, 1996, **272**, 90–92; M. P. Attfield and A. W. Sleight, *Chem. Mater.*, 1998, **10**, 2013–2019; C. Lind, A. P. Wilkinson, Z. B. Hu, S. Short and J. D. Jorgensen, *Chem. Mater.*, 1998, **10**, 2335–2337; D. A. Woodcock, P. Lightfoot, L. A. Villaescusa, M. J. Diaz-Cabanas, M. A. Camblor and D. Engberg, *Chem. Mater.*, 1999, **11**, 2508–2514; P. Lightfoot, D. A. Woodcock, M. J. Maple, L. A. Villaescusa and P. A. Wright, *J. Mater. Chem.*, 2001, **11**, 212–216; J. S. O. Evans and W. I. F. David, *Acta Crystallogr., Sect. B*, 1999, **55**, 333–340.

3 A. K. A. Pryde, K. D. Hammonds, M. T. Dove, V. Heine, J. D. Gale and M. C. Warren, *J. Phys.: Condens. Matter*, 1996, **8**, 10973–10982.

4 A. L. Goodwin and C. J. Kepert, *Phys. Rev. B*, 2005, **71**, 140301/1–140301/4.

5 A. L. Goodwin, K. W. Chapman and C. J. Kepert, *J. Am. Chem. Soc.*, 2005, **127**, 17980–17981; C. J. Kepert, *Chem. Commun.*, 2006, 695–700.

6 K. W. Chapman, P. J. Chupas and C. J. Kepert, *J. Am. Chem. Soc.*, 2005, **127**, 15630–15636; S. Margadonna, K. Prassides and A. N. Fitch, *J. Am. Chem. Soc.*, 2004, **126**, 15390–15391; S. J. Hibble, A. C. Hannon and S. M. Cheyne, *Inorg. Chem.*, 2003, **42**, 4724–4730; S. J. Hibble, S. M. Cheyne, A. C. Hannon and S. G. Eversfield, *Inorg. Chem.*, 2002, **41**, 1042–1044; D. J. Williams, D. E. Partin, F. J. Lincoln, J. Kouvetakis and M. O'Keefe, *J. Solid State Chem.*, 1997, **134**, 164–169.

7 A. P. Giddy, M. T. Dove, G. S. Pawley and V. Heine, *Acta Crystallogr., Sect. A*, 1993, **49**, 697–703; K. D. Hammonds, M. T. Dove, A. P. Giddy, V. Heine and B. Winkler, *Am. Mineral.*, 1996, **81**, 1057–1079.

8 C. James and P. S. Willand, *J. Am. Chem. Soc.*, 1916, **38**, 1497–1500; Y. Yukawa and S. Igarashi, *Inorg. Chem.*, 1996, **35**, 7399–7403; Y. Masuda, K. Nagaoka, H. Ogawa, O. Nakazato, Y. Yukawa and H. Miyamoto, *J. Alloys Compd.*, 1996, **235**, 23–29.

9 Variable temperature single crystal X-ray diffraction data of **A·4H$_2$O** were collected on a Bruker-AXS SMART 1000 CCD diffractometer and data for **A**, from dehydration of the same crystal, were collected on a Bruker-Nonius APEX II-FR591 diffractometer. Both instruments were equipped with graphite-monochromated Mo-K_α radiation and Oxford Cryosystems nitrogen cryostreams. The sample was mounted with a thin film of grease to the interior of a 0.5 mm glass capillary.

10 N. N. Greenwood and A. Earnshaw, *Chemistry of the Elements*, 2nd Edition, Butterworth-Heinemann, Oxford, UK, 1997; D. L. Kepert, *Inorganic Stereochemistry*, Springer-Verlag, Berlin, Heidelberg, New York, 1982.

11 K. W. Chapman, P. J. Chupas and C. J. Kepert, submitted.

12 A. L. Spek, *J. Appl. Crystallogr.*, 2003, **36**, 7–13.